De novo formation of an aggregation pheromone precursor by an isoprenyl diphosphate synthase-related terpene synthase in the harlequin bug

Jason Lancaster[a], Ashot Khrimian[b], Sharon Young[c], Bryan Lehner[a], Katrin Luck[d], Anna Wallingford[e], Saikat Kumar B. Ghosh[b], Philipp Zerbe[f], Andrew Muchlinski[a], Paul E. Marek[e], Michael E. Sparks[b], James G. Tokuhisa[a,g], Claus Tittiger[c], Tobias G. Köllner[d], Donald C. Weber[b], Dawn E. Gundersen-Rindal[b], Thomas P. Kuhar[e], and Dorothea Tholl[a,1]

[a]Department of Biological Sciences, Virginia Polytechnic Institute and State University, Blacksburg, VA 24061; [b]Invasive Insect Biocontrol and Behavior Laboratory, Agricultural Research Service, US Department of Agriculture, Beltsville, MD 20705; [c]Department of Biochemistry and Molecular Biology, University of Nevada, Reno, NV 89557; [d]Department of Biochemistry, Max Planck Institute for Chemical Ecology, D-07745 Jena, Germany; [e]Department of Entomology, Virginia Polytechnic Institute and State University, Blacksburg, VA 24061; [f]Department of Plant Biology, University of California, Davis, CA 95616; and [g]Department of Biochemistry, Virginia Polytechnic Institute and State University, Blacksburg, VA 24061

Edited by Rodney B. Croteau, Washington State University, Pullman, WA, and approved July 23, 2018 (received for review January 1, 2018)

Insects use a diverse array of specialized terpene metabolites as pheromones in intraspecific interactions. In contrast to plants and microbes, which employ enzymes called terpene synthases (TPSs) to synthesize terpene metabolites, limited information from few species is available about the enzymatic mechanisms underlying terpene pheromone biosynthesis in insects. Several stink bugs (Hemiptera: Pentatomidae), among them severe agricultural pests, release 15-carbon sesquiterpenes with a bisabolene skeleton as sex or aggregation pheromones. The harlequin bug, *Murgantia histrionica*, a specialist pest of crucifers, uses two stereoisomers of 10,11-epoxy-1-bisabolen-3-ol as a male-released aggregation pheromone called murgantiol. We show that *Mh*TPS (*Mh*IDS-1), an enzyme unrelated to plant and microbial TPSs but with similarity to *trans*-isoprenyl diphosphate synthases (IDS) of the core terpene biosynthetic pathway, catalyzes the formation of (1*S*,6*S*,7*R*)-1,10-bisaboladien-1-ol (sesquipiperitol) as a terpene intermediate in murgantiol biosynthesis. Sesquipiperitol, a so-far-unknown compound in animals, also occurs in plants, indicating convergent evolution in the biosynthesis of this sesquiterpene. RNAi-mediated knockdown of *MhTPS* mRNA confirmed the role of *MhTPS* in murgantiol biosynthesis. *Mh*TPS expression is highly specific to tissues lining the cuticle of the abdominal sternites of mature males. Phylogenetic analysis suggests that *Mh*TPS is derived from a *trans*-IDS progenitor and diverged from bona fide *trans*-IDS proteins including *Mh*IDS-2, which functions as an (*E*,*E*)-farnesyl diphosphate (FPP) synthase. Structure-guided mutagenesis revealed several residues critical to *Mh*TPS and *Mh*FPPS activity. The emergence of an IDS-like protein with TPS activity in *M. histrionica* demonstrates that de novo terpene biosynthesis evolved in the Hemiptera in an adaptation for intraspecific communication.

Hemiptera | Pentatomidae | harlequin bug | aggregation pheromone | terpene synthase

Terpene specialized metabolites play important roles in mediating chemical interactions of microbes, plants, and animals (1–4). In particular, volatile terpene compounds function as long- and short-distance semiochemicals in organismal interactions (5–10). Insects are well known to release volatile terpenes as interspecific signals in chemical defense or as alarm, aggregation, and sex pheromones in intraspecific communication (11–16). Despite these important functions, little is yet known about the formation of terpene specialized metabolites in insects.

In bacteria, fungi, and plants, volatile terpenes with 10-carbon (monoterpene) and 15-carbon (sesquiterpene) scaffolds are produced from the isoprenyl diphosphates, geranyl diphosphate (GPP) and farnesyl diphosphate (FPP), respectively, by enzymes called terpene synthases (TPSs) (17–23). As central intermediates in the core terpene metabolism, GPP and *trans*- or *cis*-FPP are assembled by *trans*- or *cis*-isoprenyl diphosphate synthases (IDSs) in condensations of the 5-carbon unit dimethylallyl diphosphate (DMAPP) with one or two molecules of its isomer isopentenyl diphosphate (IPP). Despite their low sequence similarity, plant- and microbial-type TPS and *trans*-IDS proteins share a common functionally active α-helical domain and catalyze reactions initiated by diphosphate ionization and carbocation formation (24–26). These structural and mechanistic similarities have led to the hypothesis of a possible ancient recruitment of IDS enzymes from core metabolism to specialized TPS function. Although insects employ a core terpene metabolism that supports juvenile hormone biosynthesis and has been associated with pheromone production (27, 28), to date no plant- or microbial-type TPS genes have been reported from insect genomes. The absence of these genes has led to the general

Significance

Many insects release volatile terpenes for chemical communication. However, the biosynthetic origin and evolution of these infochemicals are mostly unknown. We show that the harlequin bug, *Murgantia histrionica*, a stink bug pest (Hemiptera) of crucifer crops, produces a terpene aggregation pheromone by an enzyme that is unrelated to microbial and plant terpene synthases. *M. histrionica* terpene synthase activity is highly sex- and tissue-specific and makes a sesquiterpene alcohol, so far unknown in animals, as pheromone precursor. The enzyme evolved from ancestral isoprenyl diphosphate synthases and provides new evidence for de novo biosynthesis of terpenes in hemipteran insects. Knowledge of pheromone biosynthesis in stink bugs may lead to the development of new controls of these pests.

Author contributions: J.L., A.K., S.Y., B.L., A.W., S.K.B.G., P.Z., M.E.S., C.T., T.G.K., D.C.W., D.E.G.-R., T.P.K., and D.T. designed research; J.L., A.K., S.Y., B.L., K.L., A.W., S.K.B.G., A.M., M.E.S., T.G.K., and D.T. performed research; J.L., A.K., S.Y., B.L., K.L., A.W., S.K.B.G., P.Z., P.E.M., M.E.S., J.G.T., C.T., T.G.K., D.C.W., and D.T. analyzed data; and J.L., A.K., B.L., A.W., P.Z., C.T., T.G.K., and D.T. wrote the paper.

The authors declare no conflict of interest.

This article is a PNAS Direct Submission.

Data deposition: Sequences reported in this paper have been deposited in the GenBank database (accession nos. MG662378.1 for *Mh*TPS and MG662379.1 for *Mh*FPPS).

[1]To whom correspondence should be addressed. Email: tholl@vt.edu.

This article contains supporting information online at www.pnas.org/lookup/suppl/doi:10.1073/pnas.1800008115/-/DCSupplemental.

Published online August 23, 2018.

notion that insects are unable to synthesize terpene specialized metabolites de novo by the use of TPS enzymes and instead largely depend on the sequestration of terpene precursors from their host plants (15). However, studies on the biosynthesis of aggregation pheromones in Coleoptera (beetles) have shown that *trans*-IDS–like enzymes are able to convert GPP or FPP to terpene pheromones or their respective precursors. Gilg et al. (29, 30) demonstrated that the bark beetle *Ips pini* employs an IDS-like enzyme to produce the monoterpene myrcene from GPP as precursor of the aggregation pheromone ipsdienol. Recently, a similar finding has been reported from males of the flea beetle *Phyllotreta striolata*, which synthesize the cyclic sesquiterpene aggregation pheromone (6*R*,7*S*)-himachala-9,11-diene from (*Z*,*E*)-FPP by an IDS-type enzyme (31). From nine different *IDS*-type transcripts in the *P. striolata* transcriptome, two were found to encode bona fide *trans*- or *cis*-IDS enzymes, while four transcripts encode TPSs, suggesting an evolutionary origin of these enzymes from IDS progenitors. Whether insects other than beetles, especially those of earlier evolutionary origin, biosynthesize volatile terpenes de novo is unknown.

Here, we show that within the Hemiptera, stink bugs (Pentatomidae) use IDS-like proteins in pheromone biosynthesis. Several pentatomids release sesquiterpene aggregation/sex pheromones with a bisabolene carbon skeleton (32–39). Among these, the harlequin bug *Murgantia histrionica*, a crucifer specialist, produces a mixture of (3*S*,6*S*,7*R*,10*S*) and (3*S*,6*S*,7*R*,10*R*) stereoisomers of 10,11-epoxy-1-bisabolen-3-ol as a male-released aggregation pheromone dubbed murgantiol (40–42) **1** (Fig. 1). We demonstrate that an enzyme with homology to IDS proteins (*Mh*TPS) converts (*E*,*E*)-FPP **2** to sesquipiperitol **3** as the presumed stereospecific alcohol precursor of murgantiol (Fig. 1), while a second *trans*-IDS protein (*Mh*FPPS) catalyzes the formation of the *Mh*TPS substrate (*E*,*E*)-FPP from IPP and DMAPP. *MhTPS* is transcribed at high levels in males, with a predominant localization in the subcuticular tissue of the abdominal sternites. A significant role of *Mh*TPS in pheromone biosynthesis was confirmed by RNAi-mediated knockdown of *MhTPS* mRNA in *M. histrionica* males leading to reduced emission of murgantiol. Phylogenetic comparison of the *M. histrionica* enzymes with other insect IDS proteins suggests that in the Hemiptera proteins with TPS activity evolved from a *trans*-IDS progenitor. Sequence- and structure-guided mutagenesis identified several residues with critical function in *Mh*TPS and *Mh*FPPS activity. Together, our study suggests that, in comparison with

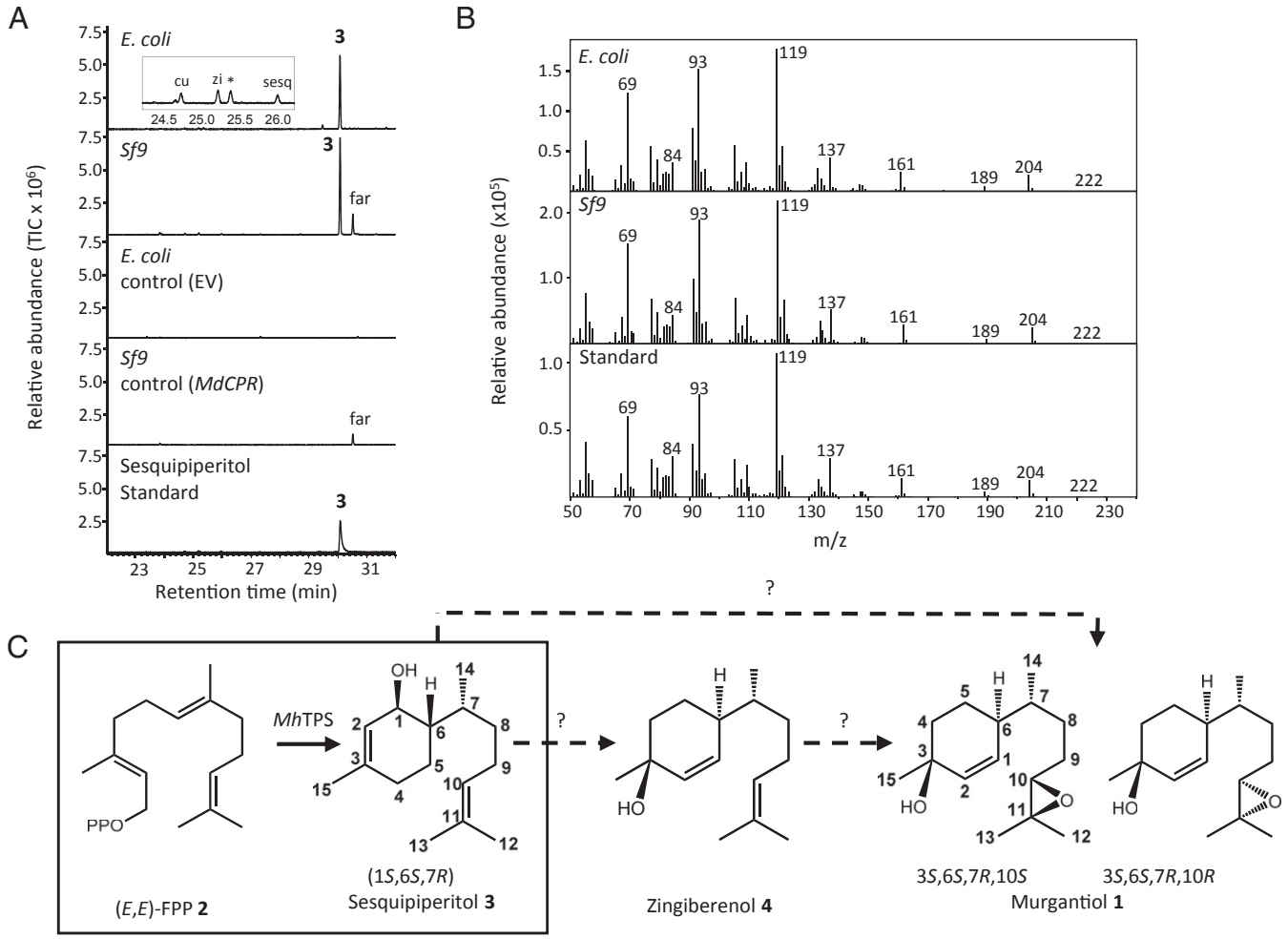

Fig. 1. Functional characterization of *MhIDS-1* (*MhTPS*) from *M. histrionica*. Recombinant *Mh*IDS-1 protein was expressed in *E. coli* and *Sf*9 cells and partially purified by affinity chromatography. Proteins were incubated with (*E*,*E*)-FPP **2** in the presence of Mg^{2+} and products were analyzed by GC-MS. (*A*) GC-MS chromatograms of enzyme products. *Sf*9 control cells express a housefly cytochrome P450 reductase. *, nonenzyme product; **3**, (1*S*,6*S*,7*R*)-sesquipiperitol; cu, γ-curcumene; far, (2*E*,6*E*)-farnesol; sesq, β-sesquiphellandrene; zi, α-zingiberene. (*B*) Mass spectra of enzymatic products with (1*S*,6*S*,7*R*)-sesquipiperitol standard **3**. (*C*) Formation of sesquipiperitol **3** by *M. histrionica* TPS activity (boxed). A putative single or two-step pathway to murgantiol **1** is shown involving isomerization and epoxidation reactions. EV, empty vector; *MdCPR*, *Musca domestica* cytochrome P450 reductase.

microbial- and plant-type TPSs, insect TPS enzymes evolved more recently from IDS proteins and this event has occurred in multiple insect lineages including hemipteran insects.

Results

Identification and Functional Characterization of *IDS*-Like Genes in *M. histrionica*. We hypothesized that in the murgantiol biosynthetic pathway of *M. histrionica* an enzyme with terpene synthase activity synthesizes a bisabolene-type hydrocarbon or alcohol terpene precursor, which presumably undergoes further modification(s) including epoxidation to form the pheromone end products (Fig. 1). To identify genes involved in the formation of the murgantiol pheromone precursor, we queried a transcriptome dataset from different sexes and developmental stages of *M. histrionica* (43) with plant and microbial TPS sequences and *trans*-IDS–type sequences of *I. pini* FPPS (AAX55631.1) and GPPS/TPS (AAX55632.1), *Bombyx mori* (silk moth) FPPS1 (NP_001036889.1) and FPPS2 (NP_001093301.1), and *Drosophila melanogaster* (fruit fly) FPPS (NP_477380). While no genes with sequence similarity to plant or microbial TPSs could be identified, two *trans*-IDS–like sequences (*MhIDS-1* and *MhIDS-2*) annotated as FPP synthase (FPPS)-like genes were retrieved. According to the transcriptome results by Sparks et al. (43), *MhIDS-1* (GECQ01420512.1; MG662378.1) mRNA levels are low in mature females but show a ∼13-fold higher accumulation in mature males, while *MhIDS-2* (GECQ01414919.1; MG662379.1) transcript levels are equal in both sexes. cDNAs of both genes were amplified from RNA extracted from mature male bugs. *MhIDS-1* encodes a 385-aa protein of 44.30 kDa while the *Mh*IDS-2 protein contains 405 aa residues and has a size of 46.36 kDa (*SI Appendix*, Fig. S1). *Mh*IDS-1 shares 22–24% sequence identity with insect FPPSs from *I. pini*, *D. melanogaster*, and the black bean aphid *Aphis fabae* (AAY33488.2), whereas comparatively higher sequence identities with these proteins (40–45%) were found for *Mh*IDS-2.

To determine the biochemical function of the detected *IDS*-like genes, cDNAs encoding full-length proteins were cloned in the bacterial protein expression vector pEXP-5, generating an N-terminal histidine-tag fusion. When tested for sesquiterpene synthase activity with (*E*,*E*)-FPP **2** as a substrate, the partially purified recombinant *Mh*IDS-1 protein produced a terpene alcohol as its main product (Fig. 1 *A* and *B*). Using GC-MS, we identified the alcohol product as sesquipiperitol **3**, a sesquiterpene alcohol with a bisabolane skeleton, which is found in different plant species (44–46). The identification of sesquipiperitol was performed by comparisons of mass spectra and retention indices and further verified by chemical correlations (Fig. 1 *A* and *B* and *SI Appendix*, *SI Results*, *SI Materials and Methods*, and Fig. S2). Sesquipiperitol was also the main product in assays upon cleavage of the N-terminal histidine tag (*SI Appendix*, Fig. S3*A*). In addition to sesquipiperitol, small and varying amounts of the sesquiterpene olefins, γ-curcumene, zingiberene, and β-sesquiphellandrene were detected (Fig. 1*A*). Hot sample injection contributed to the formation of the olefin products by thermal dehydration of sesquipiperitol, as could be shown in contrast to cool-on-column injection (*SI Appendix*, Fig. S3*B*). Sesquipiperitol was also produced, although at lower levels, from (*Z*,*E*)-FPP, but almost no enzymatic activity was found with (*Z*,*Z*)-FPP as the substrate (*SI Appendix*, Fig. S3*C*). The recombinant enzyme did further convert GPP to several monoterpenes (*SI Appendix*, Fig. S3*C*). However, when incubated with IPP and DMAPP, no formation of terpene products was observed, indicating that *Mh*IDS-1 was unable to synthesize prenyl diphosphates for subsequent conversion into terpene products (*SI Appendix*, Fig. S3*C*). Accordingly, formation of FPP by *Mh*IDS-1 was not observed. Because of its TPS activity and lack of IDS activity, we designate *Mh*IDS-1 hereinafter as *Mh*TPS. We further tested the activity of *Mh*TPS produced in insect *Sf*9 cells (Fig. 1*A*). Recombinant *Mh*TPS protein expressed without a histidine tag under these conditions generated the same enzymatic products upon incubation with (*E*,*E*)-FPP as those produced by the bacterially expressed enzyme (Fig. 1*A*). An alignment of the *Mh*TPS amino acid sequence with those of *I. pini* and *P. striolata* TPS proteins suggested the presence of a putative N-terminal targeting peptide, although the RxxS motif indicative of a mitochondrial targeting sequence is absent from the *Mh*TPS protein (*SI Appendix*, Fig. S1). Truncation of *Mh*TPS (M_1-R_{45}) resulted in the loss of enzymatic activity.

Kinetic analysis of *Mh*TPS with (*E*,*E*)-FPP as the substrate revealed an apparent K_m value of 4.0 ± 0.7 μM and a V_{max} of 675.3 ± 53.7 pkat/mg. The k_{cat} value was 0.03 ± 0.003 s^{-1} and k_{cat}/K_m was 7.5 ± 0.5 × 10^{-6} s^{-1}·mM^{-1}. K_m, k_{cat}, and k_{cat}/K_m values of *Mh*TPS1 were similar to those of plant sesqui-TPS enzymes such as (*E*)-β-caryophyllene synthase from *Artemisia annua* (47).

Recombinant *Mh*TPS1 did not produce zingiberenol **4** as a possible precursor of murgantiol. We tested whether changes in cofactor type and concentration or modifications of pH conditions would alter the enzymatic product profile and activity. No change in product specificity was observed when Mg^{2+} was substituted with Co^{2+}, although this metal ion has been found to modify product specificity of a GPP/FPP synthase in the leaf beetle *Phaedon cochleariae* (*Pc*IDS-1) (48). Activity increased by approximately twofold between 0.1 and 10 mM Mg^{2+}, while the opposite was the case for Co^{2+} (*SI Appendix*, Fig. S3*D*). Activity was highest at pH 7 (*SI Appendix*, Fig. S3*E*) and no change in product outcome was found under lower or higher pH conditions.

In contrast to *Mh*TPS1, partially purified recombinant *Mh*IDS-2 protein did not show any TPS activity when assayed with different isomers of FPP or GPP as substrates. Instead, *Mh*IDS-2 produced (*E*,*E*)-FPP from IPP and DMAPP, indicating that this protein functions as a *trans*-IDS (*SI Appendix*, Fig. S4). The enzyme was unable to synthesize any other isomer of FPP, which suggests that (*E*,*E*)-FPP is the main isomeric form produced by *M. histrionica* (*SI Appendix*, Fig. S4). Removal of a putative transit peptide (M_1-S_{58}) (*SI Appendix*, Fig. S1) led to a substantially higher production of (*E*,*E*)-FPP by the truncated *Mh*IDS-2 protein (*SI Appendix*, Fig. S4). Because of its FPPS activity, we designate *Mh*IDS-2 hereinafter as *Mh*FPPS.

Absolute Configuration of Sesquipiperitol. To further support the role of sesquipiperitol as a precursor of murgantiol, we determined the stereospecific configuration of sesquipiperitol at C-6 and C-7, which we predicted to be the same as that of murgantiol (*SI Appendix*, *SI Results*, *SI Materials and Methods*, and Figs. S2 and S5). Oxidation of enzymatically produced sesquipiperitol to sesquipiperitone **5** concluded a relative 6*S*,7*R* or 6*R*,7*S* configuration (*SI Appendix*, Fig. S2). Further conversion of sesquipiperitol to bisabolane **7** determined the configuration at C-7 to be (*R*) (*SI Appendix*, Fig. S5*A*). This result unambiguously confirmed a 6*S*,7*R* configuration of sesquipiperitol **3**, which is identical to the C-6, C-7 configuration of murgantiol **1**. Chiral GC analysis and 2D NMR recordings determined an (*S*) configuration at C-1 (*SI Appendix*, *SI Results*, *SI Materials and Methods*, and Fig. S5 *B* and *C*).

Sex- and Tissue-Specific Expression of *MhTPS*. We compared transcript abundance of *MhTPS* and *MhFPPS* between different sexes, developmental stages, and tissues by RT-PCR and qRT-PCR analyses. In agreement with mRNA levels determined by transcriptome analysis (43), *MhTPS* transcript levels were significantly higher (∼37-fold) in mature males than in mature and immature females (Fig. 2*A* and *SI Appendix*, Fig. S6*A*). *MhTPS* transcript abundance in mature males was also significantly higher than that of nymphs and immature males, which do not emit murgantiol (Fig. 2*A*). As expected from transcriptome data (43), *MhFPPS* transcript levels were comparatively higher than those of *MhTPS*

in mature females (*SI Appendix*, Fig. S6*A*). Tissue-specific transcripts of *MhTPS* localized to the tissue lining the cuticle of the abdominal sternites of mature males, while 200- to 2,000-fold lower transcript levels of *MhTPS* were observed in the thorax, fat body, and midgut (Fig. 2*B* and *SI Appendix*, Fig. S6*B*).

Sesquipiperitol Synthase Activity in *M. histrionica* Protein Extracts. To further confirm that the enzymatic activity for the formation of sesquipiperitol is present in protein lysates of *M. histrionica*, we extracted protein from the cuticle-specific tissue of mature male bugs and incubated the lysate with (*E*,*E*)-FPP. GC-MS analysis of hexane extracts obtained from the aqueous phase of the assay demonstrated the specific formation of sesquipiperitol in the presence of (*E*,*E*)-FPP (Fig. 3*A*). By contrast, protein extracts from cuticle-associated tissue of mature females did not produce sesquipiperitol, confirming the male-specific biosynthesis of this compound (Fig. 3*A*). Sesquipiperitol was not synthesized in extracts of the male head and thorax, fat body, or gut tissue when incubated with (*E*,*E*)-FPP, which further supports the tissue specificity of this enzymatic reaction (Fig. 3*B*). We did not find further conversion of sesquipiperitol to the putative downstream intermediate zingiberenol or to murgantiol or other products, suggesting that possible downstream enzymatic activities were not supported or potentially inhibited under our selected extraction and assay conditions. Alternatively, compound conversion might have been hampered by the loss of tissue integrity and compartmentalization.

Verification of in Vivo *Mh*TPS Function in Murgantiol Biosynthesis. To verify the in vivo role of *Mh*TPS in murgantiol biosynthesis, we injected males 3–5 d posteclosion with *MhTPS*-derived sequence-specific dsRNA. Transcript abundance was significantly reduced (~35- to 40-fold) 13–15 d postinjection compared with males injected with *lacZ* or Ringer's solution, or non-injected males ($P < 0.0001$) (Fig. 4*A*). Pheromone analysis of males at the same time postinjection showed significantly lower emission (approximately sevenfold) of murgantiol in *MhTPS* dsRNA males than control males (Fig. 4*B*), confirming a substantial role of *Mh*TPS in murgantiol biosynthesis.

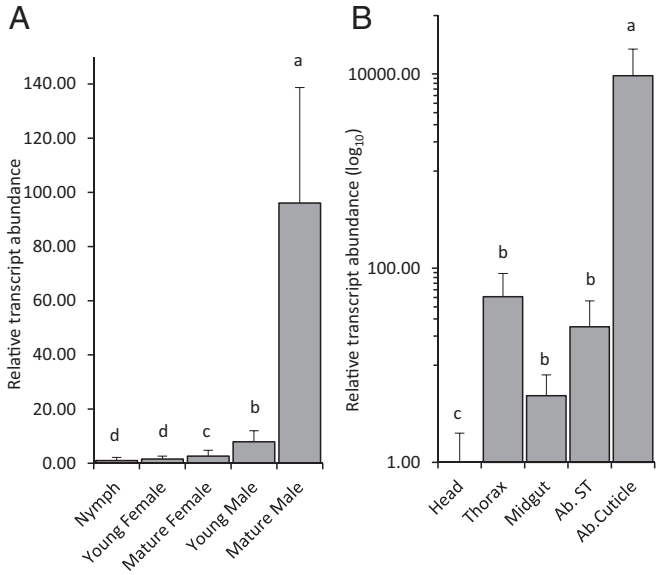

Fig. 2. Relative transcript abundance of *MhTPS* in *M. histrionica* determined by qRT-PCR. (*A*) *MhTPS* transcript abundance at different developmental stages and in different sexes. Young is 3-d adult; mature is 15-d adult. ($n = 3$, ±SD). (*B*) *MhTPS* transcript abundance in different tissues of adult males. Ab. Cuticle, tissue lining the abdominal cuticle; Ab. ST, Abdominal soft tissue minus midgut. ($n = 3$, ±SD). Gene expression was normalized against 18S rRNA. Transcript abundance is shown relative to that in nymphs (*A*) or the male head tissue (*B*) (set to 1). Significance was determined using one-way ANOVA and means grouped by Tukey's honestly significant difference test.

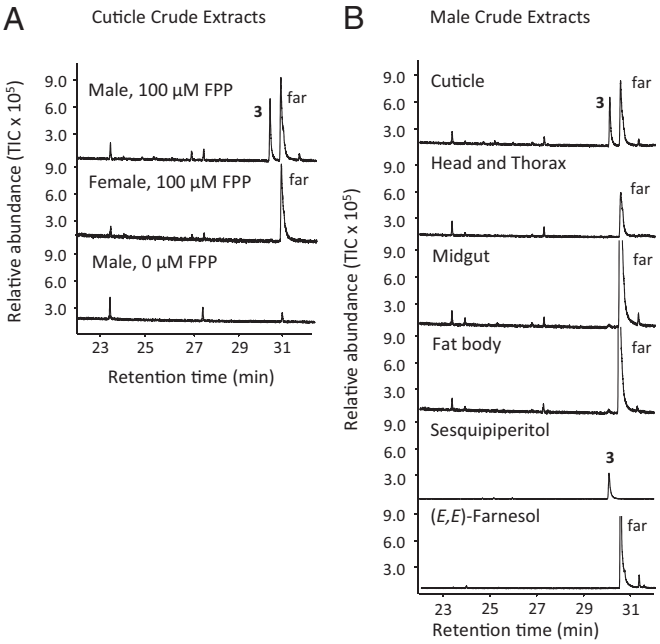

Fig. 3. Terpene synthase activity in crude protein extracts of *M. histrionica* by sex (*A*) and tissue (*B*). (*A*) Tissue of the abdominal cuticle of mature male or female *M. histrionica* was homogenized in assay buffer and assayed with 100 µM (*E*,*E*)-FPP. (*B*) Different tissues from mature male *M. histrionica* were homogenized in assay buffer and assayed with 50 µM (*E*,*E*)-FPP. Volatile products were extracted with an equal volume of hexane and analyzed with GC-MS. **3**, sesquipiperitol; far, (*E*,*E*)-farnesol.

Phylogenetic Analysis of *M. histrionica* TPS and FPPS and Determination of Residues with Function in TPS and IDS Catalytic Activity. A phylogenetic analysis based on maximum likelihood was performed to assess the evolutionary relationship of *M. histrionica* TPS and FPPS with other insect IDS and TPS enzymes (Fig. 5). The dataset included *trans*-IDS proteins from Coleoptera, Lepidoptera, and Hemiptera with known GPPS/FPPS or FPPS activities, the GPPS/TPS from *I. pini*, and the recently characterized IDS and TPS enzymes from *P. striolata*. To compare the relationship of the *M. histrionica* enzymes with similar enzymes in the Pentatomidae, we retrieved IDS-like sequences from the brown marmorated stink bug *Halyomorpha halys* based on publicly available transcriptome datasets of this insect (49). For *H. halys* two IDS-like sequences were identified, of which the IDS-1 sequence clusters with *M. histrionica* TPS (MG662378.1) (38.3% sequence identity), suggesting that *H. halys* IDS-1 might be a functional TPS enzyme. *M. histrionica* TPS and *H. halys* IDS-1 form a clade separated from *I. pini* GPPS/TPS, a *cis*-IDS (FPPS3) and the TPS clade of *P. striolata* (Fig. 5). *M. histrionica* FPPS (MG662379.1) and the more closely related *H. halys* IDS-2 protein are positioned in a larger clade of insect proteins with bona fide *trans*-FPPS or GPPS/FPPS activity from Coleoptera, Lepidoptera, and Hemiptera (Fig. 5). A broader phylogenetic analysis including insect GGPPSs and plant *trans*-IDS proteins supports an evolutionary origin of the pentatomid TPSs together with the coleopteran TPSs from a *trans*-IDS progenitor that gave rise to proteins with GPPS/FPPS or TPS activities (*SI Appendix*, Fig. S7).

BIOCHEMISTRY

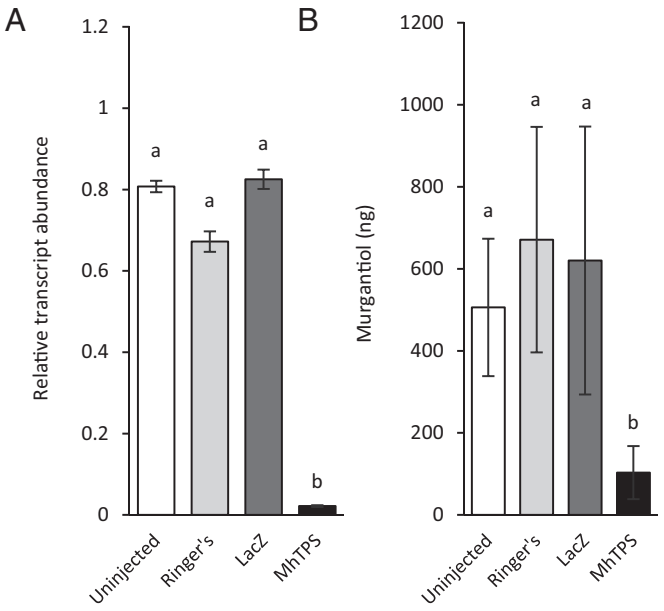

Fig. 4. Effects of RNA interference on *M. histrionica MhTPS* expression and murgantiol emission. (*A*) *MhTPS* transcript abundance in adult males 12 d postinjection normalized to 18S rRNA. *LacZ* was used as a negative control ($n = 3$, ±SEM). (*B*) Amount of murgantiol detected in headspace collections 10–12 d postinjection ($n = 9$, ±SEM). Bars in each figure with the same letter are not different according to a generalized log-linear model ($\alpha = 0.05$). (*A*) $\chi^2 = 63.13$, $P < 0.0001$. (*B*) $\chi^2 = 4883.3$, $P < 0.0001$.

Sequence comparisons between insect IDS and IDS-derived TPS enzymes show that both types of proteins contain a conserved first and second aspartate-rich motif (FARM and SARM, respectively) (*SI Appendix*, Fig. S1). These motifs are required for the coordinated binding of Mg^{2+} ions with the allylic substrate to initiate catalysis through carbocation formation and rearrangement (24–26). While residue substitutions occur in the SARM of TPSs from *I. pini* and *P. striolata*, no such substitutions are present in the TPSs of stink bugs (*SI Appendix*, Fig. S1). Notably, in comparison with bona fide *trans*-IDS proteins, the TPS proteins substitute aromatic with nonaromatic amino acid residues at positions 4 and 5 upstream of the FARM. (*SI Appendix*, Fig. S1, box M1). To determine whether these substitutions affect the orientation of (*E*,*E*)-FPP at the active site of the enzyme, we positioned (*E*,*E*)-FPP in the active site of crystallized *Gallus gallus* FPPS and an *M. histrionica* TPS homology model. This comparative positioning via ligand docking indicated that the amino acid changes upstream of the FARM (*Gg*FPPS F112, F113 – *Mh*TPS M118, S119) likely cause a different orientation of the prenyl side chain of the FPP substrate (Fig. 6*A*). Accordingly, M118F and S119F substitutions through site-directed mutagenesis resulted in the loss of TPS activity of the recombinant *Mh*TPS protein (Fig. 6*B*). By contrast, the reciprocal substitutions F95M and F96S in a truncated *Mh*FPPS protein did not abolish IDS activity but converted the enzyme into a 20-carbon geranylgeranyl diphosphate (GGPP) synthase (*SI Appendix*, Fig. S8*B*). In comparison with (*E*,*E*)-FPP, docking of DMAPP in both *Mh*TPS and *Gg*FPPS models did not result in different positions of this allylic diphosphate (*SI Appendix*, Fig. S9*A*). However, DMAPP did not have substantial inhibitory effects on the *Mh*TPS-catalyzed reaction of (*E*,*E*)-FPP to sesquipiperitol, indicating a limited affinity of the enzyme for this allylic diphosphate (*SI Appendix*, Fig. S9*B*).

To further define determinants of TPS or IDS catalytic specificity, we identified amino acids that are exclusively conserved in TPS or IDS sequences (*SI Appendix*, Fig. S1). Most of these residues were found on helices and loops outside of the predicted active side cavity of the *Mh*TPS model, making their impact on catalysis less predictable. Among residues of further interest were $S_{77}DAW_{80}$ in *Mh*TPS because these amino acids replace a highly conserved KKxR motif in *Mh*FPPS and other IDS proteins (*SI Appendix*, Fig. S1, box M2) with W80 positioned at the bottom of the active-site cavity (*SI Appendix*, Fig. S9*C*). Reciprocal substitution of these residues in *Mh*TPS and *Mh*FPPS abolished both TPS and IDS activities, indicating their critical functions in both enzymes (*SI Appendix*, Fig. S8 *A* and *B*). Loss of activity was also observed when residues $K_{135}KG_{137}$ in *Mh*TPS (K135 is a conserved amino acid in insect TPSs) were substituted with the corresponding $R_{170}PC_{172}$ sequence of full-length *Mh*FPPS, which contains a Cys residue highly conserved in insect IDS proteins (*SI Appendix*, Fig. S1, box M3). The same situation was found for the reverse mutation in *Mh*FPPS (*SI Appendix*, Figs. S1, S8 *A* and *B*, and S9*D*), again indicating critical functions of these residues in both proteins.

Discussion

***M. histrionica* TPS Functions as a Sesquiterpene Alcohol Synthase.** We found that the TPS activity associated with the recombinant *Mh*TPS enzyme and with crude lysates of male *M. histrionica* stereospecifically convert (*E*,*E*)-FPP to the (1*S*,6*S*,7*R*) isomer of sesquipiperitol **3**. The synthesis of sesquipiperitol most likely proceeds by formation of a bisabolyl cation followed by a hydride shift and subsequent quenching of the carbocation by water (*SI Appendix*, Fig. S10). The 6*S*,7*R* configuration of sesquipiperitol corroborates its function as an intermediate in the formation of

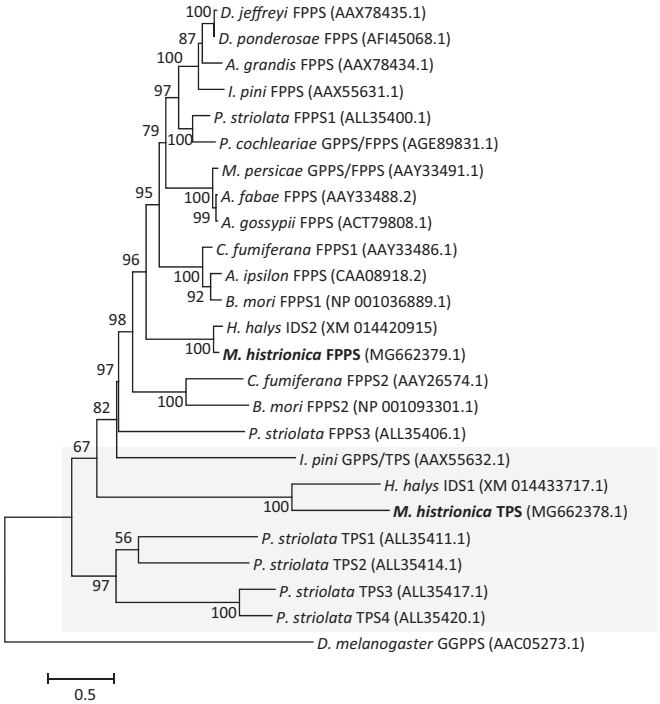

Fig. 5. Majority-rule phylogram inferred from maximum-likelihood analysis of FPPS and TPS enzymes of *M. histrionica* (bold) with related IDS proteins of *H. halys*, TPS and IDS proteins of *P. striolata*, GPPS/TPS of *I. pini*, and other insect *trans*-(GPPS)/FPPS proteins. The maximum likelihood method was based on the Le and Gascuel (59) (LG G+I) model. Bootstrap values (n = 1,000 replicates) are shown next to each node. The tree is drawn to scale, with branch lengths measured in the number of substitutions per site. Proteins with known or putative TPS activity are highlighted by the gray box. The tree was rooted using a GGPPS from *D. melanogaster*. Full species names are listed in *SI Appendix*, Fig. S7.

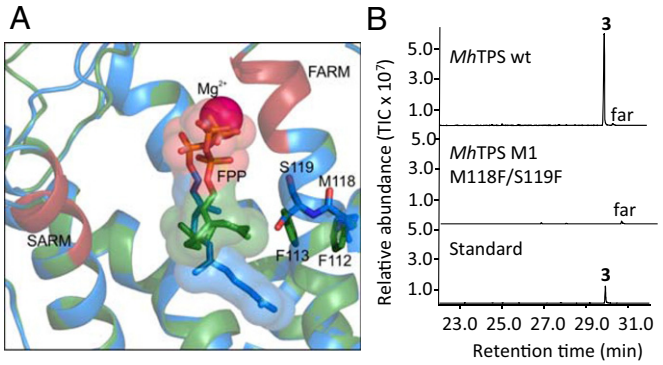

Fig. 6. Functional analysis of amino acid residues upstream of the first aspartate-rich motif of *Mh*TPS. (*A*) Position of (*E*,*E*)-FPP in the active site of *G. gallus* FPPS (green) and the *M. histrionica* TPS homology model (blue). Residues used for site-directed mutagenesis are illustrated. (*B*) TPS activity of the *Mh*TPS wild type and protein variant with residue substitutions at positions 4 and 5 upstream of the FAR motif. **3**, (1*S*,6*S*,7*R*)-sesquipiperitol; far, (*E*,*E*)-farnesol.

the murgantiol stereoisomers. An RNAi-based approach further confirmed the role of the *Mh*TPS-catalyzed reaction in murgantiol biosynthesis. The 10,11-epoxy-1-bisabolen-3-ol stereoisomers also constitute pheromone components of the brown marmorated stink bug *H. halys* (32), suggesting that the *IDS-1* gene of *H. halys* has a function similar to that of *Mh*TPS. Moreover, related TPS activities presumably operate in other pentatomids to make bisabolene-type sex pheromones or their corresponding precursors, such as isomers of zingiberenol in the rice stalk stink bug, *Tibraca limbativentris*, and the rice stink bug *Oebalus poecilus* (34, 37); the sesquiterpenes alpha-curcumene, zingiberene, and beta-sesquiphellandrene in the red-shouldered stink bug *Thyanta pallidovirens* (38); and (*Z*)-α-bisabolene epoxides in the Southern green stink bug *Nezara viridula* (33, 50). Until our finding of sesquipiperitol as an enzymatic product in *M. histrionica*, this terpenoid and its biosynthesis had not been reported in animals. The occurrence of sesquipiperitol as a natural product in different plant species (44–46) suggests convergent biosynthetic evolution of this compound by both plant- and insect-derived TPS proteins. Since several terpenes are used as identical semiochemicals by both plants and insects, it can be assumed that similar processes of convergent evolution have occurred in the synthesis of these compounds.

Terpene Formation in *M. histrionica* Is Highly Sex- and Tissue-Specific. According to the sex-specific release of murgantiol, we found the transcription of the *MhTPS* gene and its corresponding enzyme activity to be restricted to mature males. Furthermore, *Mh*TPS activity localized specifically to tissues associated with the cuticle of the abdominal sternites. The formation of the *Mh*TPS product and its conversion to murgantiol at this site would facilitate a direct release of the pheromone through pores in the abdominal cuticle. In *N. viridula*, mature males carry unicellular pheromone glands in cell layers at the ventral tissues of the abdomen, from where bisabolene epoxides are released via ducts onto the ventral abdominal surface (51). While such glands have not been observed in *M. histrionica*, *Mh*TPS activity may be located in specialized cells with precedent in the Diptera where, for example, oenocyte cells that produce cuticular hydrocarbons are in close association with the epidermis (52, 53). The site of synthesis of the terpene pheromone precursor in *M. histrionica* (abdominal cuticle) differs from that in males of the bark beetle *I. pini* (anterior midgut). Given that pheromone-biosynthesizing genes show elevated expression in male *I. pini* anterior midguts (15, 29), our findings suggest that the expression of TPS enzymes is similarly closely associated with the site of pheromone biosynthesis, but that the pheromone biosynthetic pathway can occur in different tissues depending on the modes of release of the terpene end product.

IDS-Type Terpene Synthases Evolved in the Hemiptera. Our finding of a functional TPS in *M. histrionica* suggests that adaptations of terpene-specialized metabolism for intraspecific communication have occurred in multiple lineages throughout insect evolution. To date, IDS-type TPSs with similar functions have only been characterized in the coleopterans *I. pini* and *P. striolata* (29–31). Phylogenetic analysis indicates that pentatomid and coleopteran TPSs are derived from a *trans*-IDS progenitor that diverged early from true *trans*-IDS enzymes. The separate clustering of pentatomid TPSs from *P. striolata* and *I. pini* TPSs (Fig. 5 and *SI Appendix*, Fig. S7) suggests that proteins with TPS activity might have emerged independently in these and other insect taxa. However, phylogenetic comparisons with additional TPSs from other insect lineages will be necessary to further support this hypothesis.

In our approach to identify residues that discriminate between TPS or IDS catalytic activity, we found that *Mh*TPS lost activity when nonaromatic amino acids at positions 4 and 5 upstream of the FAR motif were substituted with aromatic amino acids of equivalent position in insect IDSs. This effect was likely caused by a modified position of the FPP substrate. Molecular docking of (*E*,*E*)-FPP in the active-site cavity of an *Mh*TPS homology model showed an extension of the FPP prenyl side chain into the cavity (Fig. 6*A*), which appears to be critical for facilitating a subsequent cyclization and formation of the terpene product. For IDS enzymes, substitutions of aromatic and nonaromatic amino acids upstream of the FARM determine the chain length of the enzymatic product: nonaromatic residues facilitate the synthesis of products with extended prenyl chains in long-chain *trans*-IDS enzymes (≥C20) (54). Indeed, substitution of the two Phe residues with Met and Ser upstream of the FARM in *Mh*FPPS resulted in a change from FPPS to GGPPS activity (*SI Appendix*, Fig. S8*B*). This change in IDS product specificity correlates with the presence of nonaromatic residues in other insect GGPP synthases (55).

Loss of *Mh*TPS activity was also observed when residues $S_{77}DAW_{80}$ were substituted with KKxR, a highly conserved motif in insect IDS proteins. The charged side chain of the introduced Arg residue facing toward the hydrocarbon tail of (*E*,*E*)-FPP in this *Mh*TPS variant may prevent further cyclization (*SI Appendix*, Fig. S9*C*). The KKxR motif in insect IDSs is equivalent to the KRLR motif in the FPPS of *Escherichia coli*. The basic residues of this motif interact with the diphosphate moiety of IPP (56). Therefore, the loss of *Mh*FPPS activity by reversely substituting the KKxR motif with the SDAW sequence is most likely due to improper binding of the IPP substrate.

Reciprocal substitutions of the highly conserved Lys and Cys residues downstream of the FARM of TPS or IDS proteins, respectively, also caused a loss of activity in both mutants. Although, according to our model, these residues are positioned on a loop without immediate proximity to the docked substrate (*SI Appendix*, Fig. S9*D*), they may be involved in substrate binding and/or in the closure of the active site upon substrate binding, as has been shown, for example, for loop residues on the β-domain of TPS enzymes (57).

In summary, we were able to identify residues with critical function in TPS and IDS activity. Further structural analysis, ideally via protein crystallization and combinatorial mutations paired with the identification of epistatic residue networks (58), will be necessary to fully identify the residues controlling the transition from insect IDS to TPS enzyme activity. This evolutionary transition likely required a combination of residue substitutions to change substrate affinities and specificities for

DMAPP and IPP and gain a cyclization function following the binding of (*E*,*E*)-FPP as a single allylic substrate.

Materials and Methods

Two putative *trans*-IDS–like genes (*MhIDS-1*, *MhIDS-2*) identified in the transcriptome of *M. histrionica* were amplified as full-length cDNAs from RNA extracted from adult males and inserted in the prokaryotic expression vector pEXP5-NT/TOPO, generating an N-terminal histidine tag. A truncated version of *MhIDS-2* lacking a putative N-terminal transit peptide was cloned in the same vector, and a truncated version of *MhIDS-1* was synthesized and cloned in the pET19b expression vector. For expression in insect cells, the full-length *MhIDS-1* cDNA was cloned without an N-terminal His-tag into the BaculoDirect vector. Recombinant partially purified *Mh*IDS-1 and *Mh*IDS-2 proteins expressed in *E. coli* and lysates of *Sf*9 cells expressing *Mh*IDS-1 were tested for TPS and IDS activities and the reaction products were analyzed by GC-MS and liquid chromatography tandem MS, respectively. Identification and determination of the stereospecific configuration of the main enzymatic product of *Mh*IDS-1 (*Mh*TPS), sesquipiperitol, were performed by synthesis and chemical transformations in combination with chiral GC and NMR analysis. Kinetic properties of *Mh*TPS were examined in assays using [1-^{3}H](*E*,*E*)-FPP as substrate. Developmental, sex- and tissue-specific expression of the *MhTPS* transcript or *Mh*TPS activity were determined by qRT-PCR and TPS activity assays of crude lysates, respectively. *Mh*TPS involvement in pheromone production was verified by injecting young males of *M. histrionica* with dsRNA of *Mh*TPS or *lacZ* (control) followed by qRT-PCR and pheromone analysis in the headspace. Phylogenetic analysis was performed using maximum likelihood. *Mh*TPS and *Mh*FPPS protein variants were generated by site-directed mutagenesis, expressed in *E. coli*, and analyzed for TPS and FPPS activity. Further details on organisms, experimental and analytical procedures, data analysis, phylogenetic analysis, protein homology modeling and substrate docking are provided in *SI Appendix, SI Materials and Methods*.

ACKNOWLEDGMENTS. We thank Megan V. Herlihy and Jeremy K. Turner for assisting with harlequin bug rearing and volatile collection and Filadelfo Guzman for assisting with GC analyses. This work was supported by US Department of Agriculture National Institute of Food and Agriculture Grant 2016-67013-24759 (to D.T., D.E.G.-R., A.K., T.P.K., C.T., and D.C.W.) and the Virginia Polytechnic Institute and State University Departments of Biochemistry and Biological Sciences and the Translational Plant Sciences Program.

1. Gershenzon J, Dudareva N (2007) The function of terpene natural products in the natural world. *Nat Chem Biol* 3:408–414.
2. Osbourn A, Goss RJM, Field RA (2011) The saponins: Polar isoprenoids with important and diverse biological activities. *Nat Prod Rep* 28:1261–1268.
3. Tholl D (2015) Biosynthesis and biological functions of terpenoids in plants. *Biotechnology of Isoprenoids*, Advances in Biochemical Engineering/Biotechnology, eds Schrader J, Bohlmann J (Springer, New York), Vol 148, pp 63–106.
4. Junker RR, et al. (March 3, 2017) Covariation and phenotypic integration in chemical communication displays: Biosynthetic constraints and eco-evolutionary implications. *New Phytol*, 10.1111/nph.14505.
5. Huang M, et al. (2012) The major volatile organic compound emitted from *Arabidopsis thaliana* flowers, the sesquiterpene (*E*)-β-caryophyllene, is a defense against a bacterial pathogen. *New Phytol* 193:997–1008.
6. Raguso RA (2016) More lessons from linalool: Insights gained from a ubiquitous floral volatile. *Curr Opin Plant Biol* 32:31–36.
7. Rasmann S, et al. (2005) Recruitment of entomopathogenic nematodes by insect-damaged maize roots. *Nature* 434:732–737.
8. Robert CAM, et al. (2012) Herbivore-induced plant volatiles mediate host selection by a root herbivore. *New Phytol* 194:1061–1069.
9. Vaughan MM, et al. (2013) Formation of the unusual semivolatile diterpene rhizathalene by the *Arabidopsis* class I terpene synthase TPS08 in the root stele is involved in defense against belowground herbivory. *Plant Cell* 25:1108–1125.
10. Ditengou FA, et al. (2015) Volatile signalling by sesquiterpenes from ectomycorrhizal fungi reprogrammes root architecture. *Nat Commun* 6:6279.
11. Muller M, Buchbauer G (2011) Essential oil components as pheromones. A review. *Flavour Fragrance J* 26:357–377.
12. Sobotník J, Jirosová A, Hanus R (2010) Chemical warfare in termites. *J Insect Physiol* 56:1012–1021.
13. Burse A, et al. (2009) Always being well prepared for defense: The production of deterrents by juvenile *Chrysomelina* beetles (Chrysomelidae). *Phytochemistry* 70: 1899–1909.
14. Pickett JA, Allemannb RK, Birketta MA (2013) The semiochemistry of aphids. *Nat Prod Rep* 30:1277–1283.
15. Blomquist GJ, et al. (2010) Pheromone production in bark beetles. *Insect Biochem Mol Biol* 40:699–712.
16. Brown AE, Riddick EW, Aldrich JR, Holmes WE (2006) Identification of (-)-beta-caryophyllene as a gender-specific terpene produced by the multicolored Asian lady beetle. *J Chem Ecol* 32:2489–2499.
17. Degenhardt J, Köllner TG, Gershenzon J (2009) Monoterpene and sesquiterpene synthases and the origin of terpene skeletal diversity in plants. *Phytochemistry* 70: 1621–1637.
18. Chen F, Tholl D, Bohlmann J, Pichersky E (2011) The family of terpene synthases in plants: A mid-size family of genes for specialized metabolism that is highly diversified throughout the kingdom. *Plant J* 66:212–229.
19. Zi J, Mafu S, Peters RJ (2014) To gibberellins and beyond! Surveying the evolution of (di)terpenoid metabolism. *Annu Rev Plant Biol* 65:259–286.
20. Jia Q, et al. (2016) Microbial-type terpene synthase genes occur widely in nonseed land plants, but not in seed plants. *Proc Natl Acad Sci USA* 113:12328–12333.
21. Kumar S, et al. (2016) Molecular diversity of terpene synthases in the liverwort *Marchantia polymorpha*. *Plant Cell* 28:2632–2650.
22. Quin MB, Flynn CM, Schmidt-Dannert C (2014) Traversing the fungal terpenome. *Nat Prod Rep* 31:1449–1473.
23. Dickschat JS (2016) Bacterial terpene cyclases. *Nat Prod Rep* 33:87–110.
24. Lesburg CA, Zhai G, Cane DE, Christianson DW (1997) Crystal structure of pentalenene synthase: Mechanistic insights on terpenoid cyclization reactions in biology. *Science* 277:1820–1824.
25. Starks CM, Back K, Chappell J, Noel JP (1997) Structural basis for cyclic terpene biosynthesis by tobacco 5-epi-aristolochene synthase. *Science* 277:1815–1820.
26. Tarshis LC, Yan M, Poulter CD, Sacchettini JC (1994) Crystal structure of recombinant farnesyl diphosphate synthase at 2.6-A resolution. *Biochemistry* 33:10871–10877.
27. Bellés X, Martín D, Piulachs MD (2005) The mevalonate pathway and the synthesis of juvenile hormone in insects. *Annu Rev Entomol* 50:181–199.
28. Keeling CI, et al. (2013) Frontalin pheromone biosynthesis in the mountain pine beetle, *Dendroctonus ponderosae*, and the role of isoprenyl diphosphate synthases. *Proc Natl Acad Sci USA* 110:18838–18843.
29. Gilg AB, Bearfield JC, Tittiger C, Welch WH, Blomquist GJ (2005) Isolation and functional expression of an animal geranyl diphosphate synthase and its role in bark beetle pheromone biosynthesis. *Proc Natl Acad Sci USA* 102:9760–9765.
30. Gilg AB, Tittiger C, Blomquist GJ (2009) Unique animal prenyltransferase with monoterpene synthase activity. *Naturwissenschaften* 96:731–735.
31. Beran F, et al. (2016) Novel family of terpene synthases evolved from trans-isoprenyl diphosphate synthases in a flea beetle. *Proc Natl Acad Sci USA* 113:2922–2927.
32. Khrimian A, et al. (2014) Discovery of the aggregation pheromone of the brown marmorated stink bug (*Halyomorpha halys*) through the creation of stereoisomeric libraries of 1-bisabolen-3-ols. *J Nat Prod* 77:1708–1717.
33. Aldrich JR, et al. (1993) Artifacts and pheromone blends from *Nezara* spp. and other stink bugs (Heteroptera, Pentatomidae). *Z Naturforsch C Biosci* 48:73–79.
34. Borges M, et al. (2006) Sex attractant pheromone from the rice stalk stink bug, *Tibraca limbativentris* Stal. *J Chem Ecol* 32:2749–2761.
35. Moraes MCB, Pareja M, Laumann RA, Borges M (2008) The chemical volatiles (semiochemicals) produced by neotropical stink bugs (Hemiptera: Pentatomidae). *Neotrop Entomol* 37:489–505.
36. Blassioli-Moraes MC, et al. (2012) Sex pheromone communication in two sympatric neotropical stink bug species *Chinavia ubica* and *Chinavia impicticornis*. *J Chem Ecol* 38:836–845.
37. de Oliveira MWM, et al. (2013) Zingiberenol, (1*R*,4*R*,1′*S*)-4-(1′,5′-Dimethylhex-4′-enyl)-1-methylcyclohex-2-en-1-ol, identified as the sex pheromone produced by males of the rice stink bug *Oebalus poecilus* (Heteroptera: Pentatomidae). *J Agric Food Chem* 61:7777–7785.
38. McBrien HL, et al. (2002) Sex attractant pheromone of the red-shouldered stink bug *Thyanta pallidovirens*: A pheromone blend with multiple redundant components. *J Chem Ecol* 28:1797–1818.
39. Weber DC, Khrimian A, Blassioli-Moraes MC, Millar JG (2018) Semiochemistry of Pentatomoidea. *Invasive Stink Bugs and Related Species (Pentatomoidea): Biology, Higher Systematics, Semiochemistry, and Management*, ed McPherson JE (CRC, Boca Raton, FL), pp 677–725.
40. Khrimian A, et al. (2014) Determination of the stereochemistry of the aggregation pheromone of harlequin bug, *Murgantia histrionica*. *J Chem Ecol* 40:1260–1268.
41. Weber DC, et al. (2014) Attractiveness of harlequin bug, *Murgantia histrionica*, aggregation pheromone: Field response to isomers, ratios, and dose. *J Chem Ecol* 40: 1251–1259.
42. Zahn DK, Moreira JA, Millar JG (2008) Identification, synthesis, and bioassay of a male-specific aggregation pheromone from the harlequin bug, *Murgantia histrionica*. *J Chem Ecol* 34:238–251.
43. Sparks ME, et al. (2017) A transcriptome survey spanning life stages and sexes of the harlequin bug, *Murgantia histrionica*. *Insects* 8:55.
44. Bohlmann F, Tsankova E, Jakupovic J (1984) Sesquiterpenes and acetylenes from *Argyranthemum adauctum* ssp. *jacobaeifolium*. *Phytochemistry* 23:1103–1104.
45. Sy LK, Brown GD (1997) Oxygenated bisabolanes from *Alpinia densibracteata*. *Phytochemistry* 45:537–544.
46. Cool LG (1996) Sesquiterpene alcohols from foliage of *Fitzroya cupressoides*. *Phytochemistry* 42:1015–1019.
47. Cai Y, et al. (2002) A cDNA clone for beta-caryophyllene synthase from *Artemisia annua*. *Phytochemistry* 61:523–529.
48. Frick S, et al. (2013) Metal ions control product specificity of isoprenyl diphosphate synthases in the insect terpenoid pathway. *Proc Natl Acad Sci USA* 110:4194–4199.
49. Sparks ME, Shelby KS, Kuhar D, Gundersen-Rindal DE (2014) Transcriptome of the invasive brown marmorated stink bug, *Halyomorpha halys* (Stål) (Heteroptera: Pentatomidae). *PLoS One* 9:e111646.

50. Aldrich JR, Oliver JE, Lusby WR, Kochansky JP, Lockwood JA (1987) Pheromone strains of the cosmopolitan pest, *Nezara viridula* (Heteroptera, Pentatomidae). *J Exp Zool* 244:171–175.
51. Cribb BW, Siriwardana KN, Walter GH (2006) Unicellular pheromone glands of the pentatomid bug *Nezara viridula* (Heteroptera: Insecta): Ultrastructure, classification, and proposed function. *J Morphol* 267:831–840.
52. Qiu Y, et al. (2012) An insect-specific P450 oxidative decarbonylase for cuticular hydrocarbon biosynthesis. *Proc Natl Acad Sci USA* 109:14858–14863.
53. Martins GF, Ramalho-Ortigao JM (2012) Oenocytes in insects. *Invert Surviv J* 9:139–152.
54. Wallrapp FH, et al. (2013) Prediction of function for the polyprenyl transferase subgroup in the isoprenoid synthase superfamily. *Proc Natl Acad Sci USA* 110:E1196–E1202.
55. Lai C, McMahon R, Young C, Mackay TFC, Langley CH (1998) quemao, a *Drosophila* bristle locus, encodes geranylgeranyl pyrophosphate synthase. *Genetics* 149: 1051–1061.
56. Hosfield DJ, et al. (2004) Structural basis for bisphosphonate-mediated inhibition of isoprenoid biosynthesis. *J Biol Chem* 279:8526–8529.
57. Christianson DW (2017) Structural and chemical biology of terpenoid cyclases. *Chem Rev* 117:11570–11648.
58. Salmon M, et al. (2015) Emergence of terpene cyclization in *Artemisia annua*. *Nat Commun* 6:6143.
59. Le SQ, Gascuel O (2008) An improved general amino acid replacement matrix. *Mol Biol Evol* 25:1307–1320.